Synthesis, Rodent Biodistribution, Dosimetry, Metabolism, and Monkey Images of Carbon-11-Labeled (+)-2α-Tropanyl Benzilate: A Central Muscarinic Receptor Imaging Agent

G. Keith Mulholland,* Charlotte A. Otto,† Douglas M. Jewett,* Michael R. Kilbourn,* Robert A. Koeppe,* Phillip S. Sherman,* Neil A. Petry,* James E. Carey,* Edward R. Atkinson,‡ Sydney Archer,§ Kirk A. Frey* and David E. Kuhl*

*Division of Nuclear Medicine, University of Michigan, Ann Arbor, Michigan; †University of Michigan-Dearborn, Dearborn, Michigan; ‡Amherst, Massachusetts; and §Department of Chemistry, Rensselaer Polytechnic Institute, Troy, New York

Muscarinic cholinergic receptors (mAChR) are abundant in the brain, and the mAChR system mediates many aspects of brain function. There is evidence of alterations in muscarinic binding in degenerative brain disorders. A muscarinic receptor radioligand, carbon-11-(+)-2α-tropanyl benzilate ([^{11}C]TRB), has been prepared through N-[^{11}C]methylation of N-desmethyl TRB, and evaluated in rodents and primates. Full body biodistribution in rats has been determined and the expected human dosimetry calculated. Comparisons with [^{11}C]scopolamine in rats showed 2–6 times greater brain uptake of [^{11}C]TRB. Highly specific and saturable binding of [^{11}C]TRB in the striatum and cortex was demonstrated by greater than 85% blockade of uptake following QNB or scopolamine pretreatment. Striatum/cerebellum ratios in mice at 60 min exceeded 12.6. TLC analysis of rat tissues showed the absence of ^{11}C-metabolites in brain and heart, and a rapid solid phase C-18 Sep-Pak method found that unmetabolized plasma [^{11}C]TRB in monkeys fell from 81% at 5 min to 48% at 80 min. Finally, brains of living primates have been imaged using PET and [^{11}C]TRB; regional localization was consistent with muscarinic receptor distribution. These results represent intermediate steps in the development of [^{11}C]TRB for quantification of central muscarinic receptors in man.

J Nucl Med 1992; 33:423–430

Muscarinic cholinergic receptors (mAChR) are abundant in the brain, particularly in striatal and cortical areas, and the mAChR system mediates many aspects of brain function, including higher processes of cognition and memory. There is evidence of alterations in muscarinic binding in degenerative brain disorders such as Alzheimer's, Huntington's, and Parkinson's disease (*1–6*). For these reasons, there has been considerable interest in studying the regional distribution of central muscarinic cholinergic binding sites in man with labeled receptor binding drugs and external imaging techniques. A number of high affinity radiolabeled muscarinic antagonists have been prepared for investigation as potential muscarinic imaging agents, including quinuclidinyl benzilate (QNB) analogs labeled with radioiodine (*7–11*) and ^{11}C (*12*), dexetimide analogs containing radioiodine (*13*), ^{11}C (*14*), and ^{18}F, (*15, 16*), [^{11}C]scopolamine (*17,18*) and [^{11}C]benztropine (*19–21*). There has been particular interest in using positron emission tomography (PET) with an appropriate muscarinic ligand because of the hope that this technique's high resolution and ability for noninvasive quantification of radioactivity distribution in the living human brain will provide new information concerning relationships between mAChR activity and brain functional status in disease and in health.

In connection with ongoing efforts to study mAChR with PET (*18,22*), we have recently examined [^{11}C]scopolamine in humans (*23*). The present work stems from our search for alternate mAChR radioligands with more favorable tracer characteristics and more convenient synthetic access than scopolamine (*24*). A preliminary part of this search involved in vitro and ex vivo screening of a group of candidate antimuscarinic benzilate ester ligands in unlabeled forms for muscarinic specificity, binding affinity and brain penetration (*25*). From this group of compounds (+)2α-tropanyl benzilate (TRB) (Scheme 1), a potent centrally active mAChR antagonist (*26*), was selected for radiosynthesis and further study. Here the biological properties of [^{11}C]TRB are examined in rodents and nonhuman primates, and some comparisons between the rodent data of [^{11}C]TRB and [^{11}C]scopolamine are made. These results represent intermediate steps toward

Received May 15, 1991; revision accepted Oct. 31, 1991.

For reprints contact: G. Keith Mulholland, PhD, University of Michigan, Division of Nuclear Medicine, Cyclotron/PET Facility, 3480 Kresge III, Ann Arbor, MI 48109.

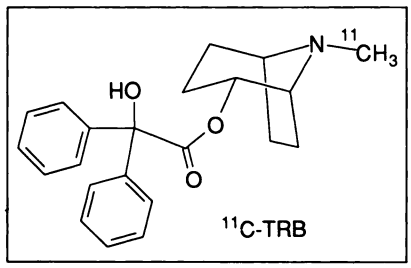

SCHEME 1. Structure for [^{11}C]TRB.

development of [^{11}C]TRB as a radiopharmaceutical for mapping central mAChRs in man.

METHODS

Chemistry

N-Desmethyl TRB and authentic TRB were prepared by methods described previously (*26,27*). Carbon-11-labeled methyl iodide was prepared from [^{11}C]CO_2 by modification of published methods (*28*). Carbon-11-scopolamine was prepared by reductive [^{11}C]methylation of norscopolamine with [^{11}C]formaldehyde (*18*).

Carbon-11-TRB was labeled by [^{11}C]methyl iodide N-[^{11}C] methylation of desmethyl TRB, using an apparatus similar in design to the one used for synthesis of [^{11}C]scopolamine (*18*). Gaseous [^{11}C]methyl iodide was bubbled into a reaction solution of 1.5 mg of desmethyl TRB and 5 μl of diisopropylethylamine in 200 μl of dimethylformamide cooled to −50° in a conical vial. The reaction vial was sealed and heated at 80° for 4 min, and then 600 μl of water were added. The diluted reaction solution was passed through a short solid-phase extraction column of C-18 silica which retained the crude product [^{11}C]TRB. This column was then rinsed with water (2 × 1 ml) and dried for 1 min by a high pressure flow of helium (10 bar). The adsorbed crude product was eluted from the extraction column onto a 9.6 × 150 mm amino/cyano bonded phase 5 micron silica semipreparative HPLC column (ES Industries, Marlton, NJ) by a 3-ml/min flow of chromatographic solvent (93:7 acetonitrile: isopropanol). After separation of [^{11}C]TRB (retention time 7 min) from excess precursor desmethyl TRB (10 min) was effected, the solvent was removed from the [^{11}C]TRB fraction by rotary evaporation and the final product was formulated in isotonic saline containing 10% ethanol. The chemical and radiochemical purity, and specific activity of each batch of [^{11}C]TRB was assayed by analytical HPLC using series ultraviolet (220 nm) and radioactivity flow detectors. Column: 4.6 × 250 mm 5 μm C-18; solvent: 3:1:1 acetonitrile: methanol: 20 m*M* pH 6.7 $KHPO_4$, 1 ml/min; k'_{TRB} 1.8, $k'_{desmethyl\ TRB}$ 1.6. The limit of mass detection of these two components under routine conditions was 0.2 μg/ml of formulated product solution. Typical specifications for batches of [^{11}C] TRB were as follows: radiochemical purity: >99%; specific activity at end of synthesis: 0.5 − 3 Ci/μmol. The amount of desmethyl TRB in the final product ranged from none detectable to 20% of the mass of TRB present. The time required for synthesis and formulation of [^{11}C]TRB was 33–45 min, the end of synthesis yield was 250–320 mCi (20 μA/20 min target irradiation), and the decay-corrected yield based on [^{11}C]CO_2 was 50%–70%.

Rodent Distribution

Female Sprague Dawley (SD) rats weighing 175–200 g were used in the regional brain distribution studies. A separate set of SD rats of both sexes were used for whole-body biodistribution and dosimetry studies. Rats were anesthetized with ethyl ether and [^{11}C]TRB was injected into the femoral vein at doses of 150–900 μCi in 250 μl of formulated solution. The approximate injected mass of TRB was between 0.3–6 nmol/kg. Animals were allowed to recover from anesthesia after tracer injection and normal activity was resumed until the time of sacrifice. Animals were killed by decapitation at specific times and whole tissues were dissected out, counted for ^{11}C in a NaI(Tl) well counter, and weighed. Brains were dissected into the following regions: striatum, cerebral cortex (entire), cerebellum, in some cases pons-medulla, and rest of brain. The carcass was measured for radioactivity in a dose calibrator. Results were corrected for radioactive decay. They were calculated in terms of percent of injected dose per organ (%ID/organ), and percent of injected dose per gram of wet tissue, normalized to a hypothetical animal body weight of 1 kg (kg %ID/g), to correct for individual animal weight differences and allow for cross-species comparisons of distribution data. The number of animals used in each time point are indicated in the figure or table where the data are presented. Results for each data point are expressed as the mean value plus or minus the standard deviation. Carbon-11-scopolamine rat studies were carried out at similar mass and radioactivity doses and conditions. Brain [^{11}C] TRB radioactivity distribution was also examined in a group of 11 mixed-sex C57BL/6 mice, 20–30g, at 60 min following 50–100 μCi i.v. (tail vein) doses of [^{11}C]TRB.

In blocking studies to demonstrate the degree of muscarinic specificity of TRB uptake in various tissues, animals were injected subcutaneously with either (±)QNB, 2 mg/kg, (−)scopolamine, 8 mg/kg, or saline vehicle alone, 60–90 min prior to tracer injection.

Rat Tissue Metabolite Assay

Carbon-11-TRB (5 mCi) was injected via the femoral vein into a 190-g female SD rat. Blood samples (250 μl) were collected in tubes containing 10 mg of potassium fluoride at 10 and 20 min following tracer injection. At 30 min, the rat was killed and a third blood sample (1 ml) was collected. Brain, heart, small intestine and pancreas were quickly removed, minced, and then homogenized with 3 ml of ethanol containing 10% acetic acid. Whole blood samples were shaken briefly with three volumes of the same ethanol/acetic acid extractant. Each tissue mixture was then centrifuged, counted, and the supernatant extract was separated from the cell debris. The cell debris was shaken with 3 ml of pure ethanol, centrifuged, and the second extract removed and combined with the first. The debris was extracted once more, the residue and pooled extracts for each tissue were counted to determine recovery efficiency, and the extract was reduced to <0.5 ml total volume on a rotary evaporator. Aliquots of the resulting concentrate were applied to glass-backed silica thin-layer chromatography plates (E. Merck, 15 cm) and developed with a solvent mixture containing CH_2Cl_2:Et_2O:Et_3N: EtOH, 10:10:1:1. This system clearly separates TRB (R_f 0.65) and desmethyl TRB (R_f 0.4). Chromatogram radioactivity was examined with a Berthold linear analyzer. The experiment was repeated with a second rat in which only the brain, heart, and small intestine were examined.

Monkey PET Imaging

Qualitative images of brain radioactivity distribution were conducted in female pigtail monkeys (*Macaca nemistrina*) weighing 6–7 kg, (n = 3) and a 15-kg female baboon (*Papio anubis*) (n

= 2), using the TCC 4600A three-ring, five-slice PET camera with a resolution of 13 mm FWHM. Animals were anesthetized with intramuscular ketamine (15 mg/kg), and xylazine hydrochloride (2 mg/kg), and they were intubated to prevent aspiration of salivary secretions. Ketamine was repeated as necessary to maintain anesthesia. Heads were positioned in an acrylic head holder with a bite bar and Velcro straps. After a preliminary [^{15}O]H_2O scan for positioning and to assure normal blood flow, [^{11}C]TRB, 1–1.5 mCi/kg (0.9–6 nmol/kg), was injected intravenously. Kinetic data were acquired using an 18 frame acquisition sequence which lasted between 65–120 min in duration. Studies ran 120 min unless terminated by equipment or animal difficulties. Venous blood was sampled periodically for metabolites (see below). A mathematical attenuation correction was applied in image reconstruction. Regions of interest were drawn around the striatum/frontal cortex (separation was indistinct), temporal cortex and cerebellum. Ipsolateral regions were compared whenever possible to minimize the effects of side-to-side head motion.

To examine the effect of pharmacological levels of scopolamine on brain [^{11}C]TRB levels in the baboon, 20 mCi of [^{11}C]TRB was administered intravenously in a 5-ml bolus at the beginning of a 120-min scan. At 110 min, scopolamine 200 μg/kg (0.67 μmol/kg), was administered intravenously and the baboon's heart rate was monitored. Twenty minutes after the mild tachycardia due to scopolamine had subsided, a second 120-min scan was carried out using another 20 mCi injection of [^{11}C]TRB with the same specific activity as the first dose.

Primate Blood Plasma Metabolite Assay

An anesthetized female pigtail monkey weighing 7 kg was given an intravenous injection of 10 mCi of [^{11}C]TRB. Blood samples were collected in tubes containing 10 mg of potassium fluoride (to minimize coagulation) at 5, 10, 20, 30, 40 min (500 μl), 60 and 80 min (1 ml), and centrifuged for 1 min. The plasma was separated with a pipet and applied to a C-18 Sep-Pak preconditioned with 5 ml of methanol followed by 10 ml of 1% aqueous ammonium carbonate. A 15-ml portion of 1% aqueous ammonium carbonate was passed through the Sep-Pak after the plasma and the aqueous eluent (soluble metabolite fraction) was collected. The Sep-Pak was then washed with 15 ml of ethanol to elute the [^{11}C]TRB fraction. The red blood cell pellet, eluent fractions, and Sep-Pak after final rinse were counted for ^{11}C. The recovery efficiency for TRB of this assay was determined in control experiments using primate whole blood spiked with authentic [^{11}C]TRB. Total unmetabolized [^{11}C]TRB in plasma was calculated as the activity in the ethanol fraction times a recovery correction factor of 1.03 to compensate for TRB irreversibly bound to the Sep-Pak. The ability of this assay to separate [^{11}C]TRB and metabolites was checked using rat blood metabolites, with the assumption made that monkey and rat metabolites were the same chromatographically. Blood samples (5 and 60 min) from two more monkey studies in the same animal on different occasions were assayed by this procedure and these results did not vary from the first by more than 10%.

RESULTS

Rodent Distribution

The regional brain concentrations of [^{11}C]TRB in rats and mice at various time points up to 90 min postinjection are shown in Table 1. Rat cerebellum concentrations peaked within the first 2 min and then declined. Whole cortex and striatum values were stable or continued to rise gradually over the 90-min period. Brain region-to-blood activity ratios at 90 min ranged from about 3 for cerebellum to 30 for striatum. The brain localization of [^{11}C]TRB in mice was consistent with rat data, showing similar striatum-to-cerebellum ratios and %ID/brain values. The full body rat [^{11}C]TRB radioactivity distribution (%ID/organ) in a separate set of rats is shown in Table 2. Decay-corrected radioactivity in most tissues peaked within the first 15 min, with liver, lung and kidney containing large amounts of radioactivity early on. By 15 min, the brain contained the highest total amount of activity after the liver and remained so thereon. About 80% of the total administered radioactivity could be accounted for in the organs and carcass (includes intestinal contents but not urine) 90 min after injection.

The 30-min uptake of [^{11}C]TRB in rat tissues under control conditions or with QNB or scopolamine pretreatment are shown in Table 1 and Figure 1A. Similar degrees of uptake inhibition were observed using either pretreat-

TABLE 1
Regional Brain Distribution of [^{11}C]TRB in Rodents

Tissue kg% dose/g*	Rat (n = 3–5)							Mouse (n = 11)
	2 min	20 min	30 min	30 min	30 min	60 min	90 min	60 min
Striatum	0.37 ± 0.05	0.62 ± 0.076	0.52 ± 0.02	0.061 ± 0.008	0.064 ± 0.002	0.71 ± 0.097	0.74 ± 0.04	0.326 ± 0.042
Cortex (whole)	0.41 ± 0.075	0.72 ± 0.043	0.52 ± 0.04	0.062 ± 0.008	0.071 ± 0.006	0.61 ± 0.07	0.59 ± 0.061	0.262 ± 0.069
Cerebellum	0.23 ± 0.05	0.17 ± 0.015	0.1 ± 0.009	0.045 ± 0.005	0.051 ± 0.004	0.084 ± 0.012	0.072 ± 0.005	0.025 ± 0.003
Blood	0.048 ± 0.001	0.026 ± 0.005	0.02 ± 0.001	0.019 ± 0.002	0.027 ± 0.002	0.022 ± 0.002	0.024 ± 0.002	0.015 ± 0.001
Striatum/ Cerebellum	1.7 ± 0.24	3.69 ± 0.25	5.4 ± 0.52	1.34 ± 0.06	1.26 ± 0.17	8.49 ± 0.42	10.3 ± 0.6	12.7 ± 3.2
%ID/brain	2.93 ± 0.45	4.03 ± 0.31	3.7 ± 0.47	0.57 ± 0.053	0.66 ± 0.006	3.34 ± 0.27	3.11 ± 0.5	4.29 ± 0.06

* Data are given as the mean ± standard deviation.

TABLE 2
Whole Body Biodistribution of [^{11}C]TRB in Rats*

	%Injected dose per organ			
	2 min	15 min	45 min	90 min
Brain	3.78 ± 0.53	5.77 ± 0.77	4.06 ± 0.39	3.34 ± 0.16
Heart	1.40 ± 0.16	1.26 ± 0.08	0.76 ± 0.08	0.31 ± 0.07
Kidney	7.31 ± 1.11	3.18 ± 0.56	2.27 ± 0.72	0.74 ± 0.19
Liver	14.6 ± 2.71	9.72 ± 0.85	9.09 ± 1.34	6.71 ± 1.38
Lung	8.47 ± 1.30	2.99 ± 0.50	1.83 ± 0.32	0.41 ± 0.08
Testes	0.78 ± 0.05	1.08 ± 0.14	0.86 ± 0.043	0.87 ± 0.03
Spleen	1.03 ± 0.51	0.80 ± 0.12	0.38 ± 0.033	0.15 ± 0.05
Ovary	0.22 ± 0.003	0.09 ± 0.02	0.06 ± 0.015	0.02 ± 0.005
Carcass	73.7 ± 10.3	68.7 ± 6.25	68.0 ± 5.46	67.14 ± 4.17
Total	110 ± 12.0	92.4 ± 5.64	87.1 ± 4.28	79.5 ± 3.8

* Data are given as mean ± standard deviation. n = 5–6 rats per data point.

ment drug, with the greatest reductions seen in the striatum and cortex (86%–88%) followed by the ponsmedulla (82%) and cerebellum (50%). More than 80% of the heart uptake of [^{11}C]TRB could be blocked by QNB (Fig. 1A).

Comparison with [^{11}C]Scopolamine

Rat tissue radioactivity levels 30 min after tracer injection under control conditions and following blocking pretreatment with "cold" QNB are shown for [^{11}C]TRB and [^{11}C]scopolamine in Figure 1. Tracer uptake in tissues containing muscarinic receptors was substantially greater in the case of [^{11}C]TRB. Overall control brain levels of [^{11}C]TRB were two-fold greater than [^{11}C]scopolamine at 2 min and approximately six times greater than [^{11}C] scopolamine brain levels at 90 min (n = 3–5 animals/time point: data not shown). The percent reduction of control uptake seen after QNB pretreatment was similar with both [^{11}C]TRB and [^{11}C]scopolamine.

Dosimetry Estimates

The expected absorbed doses to humans for a 50-mCi dose of [^{11}C]TRB are shown in Table 3. The dose-limiting organ was the ovary. Dosimetry data were calculated using the rat biodistribution data from Table 2 following the MIRD formalism (*29*). The percent administered dose per organ values were modified to reflect the different proportions of organ to total body mass in rat and man (*30*). Residence times were obtained by integration under the organ time versus activity curves, with the effective half-life of [^{11}C]TRB assumed to be equal to the physical half-life of ^{11}C for times exceeding the last data point. Residence times were entered into the MIRDOSE2 program (*31*) for the generation of absorbed doses to selected target organs per unit of administered activity.

TABLE 3
Calculated Absorbed Dose Estimates to the Adult from [^{11}C]TRB

Target organ	rad/mCi*	Total rad/ 50 mCi
Brain	0.0426	2.13
Heart wall	0.0432	2.16
Kidneys	0.0382	1.91
Liver	0.0212	1.06
Lungs	0.0495	2.48
Ovaries	0.0353	1.77
Red marrow	0.0115	0.58
Spleen	0.0245	1.23
Testes	0.0082	0.41
Total body	0.0011	0.06

Metabolism Experiments

Thin-layer chromatographic (TLC) examination of rat brain extracts found at least 97% of extractable brain radioactivity to be identical to unmetabolized TRB. The recovery efficiency of the three-step extraction procedure with brain tissue was 86% and 83% respectively for two rats. Heart and pancreas extracts (recovery ~90%) likewise showed a single radioactive species coincident with authentic TRB, indicating no radioactive metabolite accumulation in these tissues either. Small intestine homogenates yielded the lowest recovery (76%) of extractible radioactivity of the tissues examined, and in contrast to the above tissues, the intestinal extract was predominantly (75% and 90% in the two rats) a single highly polar metabolite fraction which did not migrate from the origin.

Rat whole blood examined by the extraction-TLC method (90%–95% recovery) at 10 min following tracer injection showed 83% unmetabolized TRB. The balance of plate radioactivity was highly polar. The unmetabolized fractions of recovered radioactivity in rat blood at 20 and 30 min were approximately 65% and 50%, respectively.

The results of Sep-Pak analysis of sequential samples of venous plasma from one monkey following [^{11}C]TRB are shown in Figure 2. Control experiments found 56% of spiked authentic [^{11}C]TRB in whole blood partitioned into the plasma after centrifugation. The percentage of total blood radioactivity (TRB plus metabolites) that partitioned into plasma upon centrifugation was invariant over the seven time points assayed, with a mean partition value of 55% ± 2%. About 97% of authentic [^{11}C]TRB in plasma

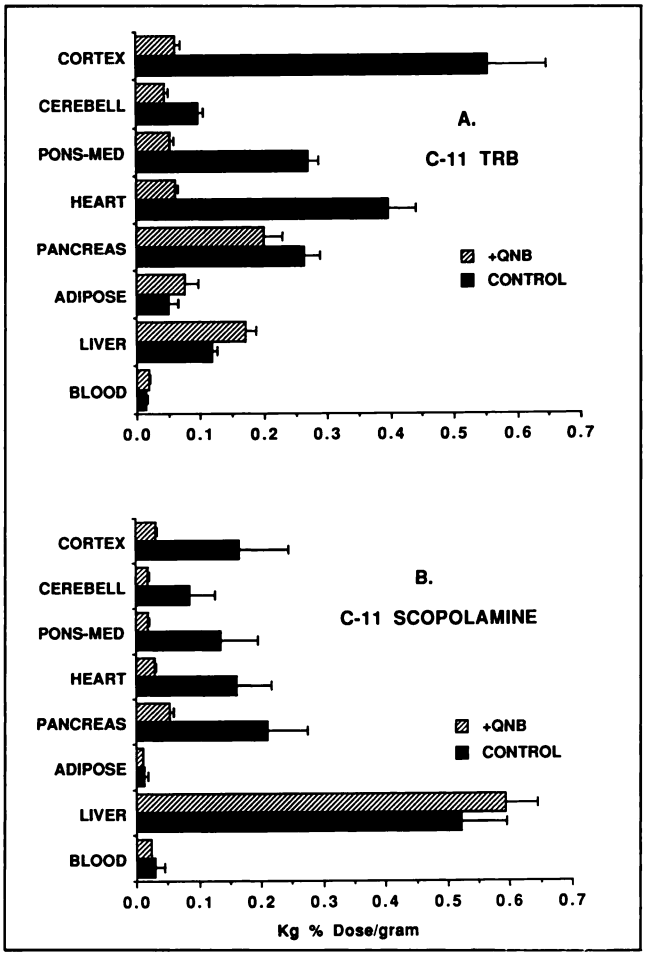

FIGURE 1. Radioactivity levels in selected rat tissues in control and QNB pretreated conditions, 30 min following intravenous injection of [^{11}C]TRB (A) or [^{11}C]scopolamine (B). Each data point represents the mean ± standard deviation of at least three animals.

was recovered in the ethanol fraction by the Sep-Pak assay. Authentic [^{11}C]TRB activity and labeled metabolites were weakly associated to the red blood cells (RBC), and most RBC activity could be recovered in an additional step which involved resuspending cells in 1.5 ml of pH 6.7 phosphate-buffered saline, recentrifugation and collection of the supernatant. When this second step was carried out on the RBCs from the 40-min sample, Sep-Pak analysis of the resulting supernatant showed the same ratio of metabolites to TRB as in the first supernatant. This indicated that selective partitioning of radiolabeled species between RBCs and plasma did not occur significantly and thus it is reasonable to assume the metabolite fraction of [^{11}C] TRB measured in plasma by this assay accurately reflects the true metabolite fraction in whole blood.

Monkey PET Images

A representative late image of [^{11}C]TRB distribution in the baboon brain is shown in the top row of Figure 3. Activity was highest in areas anatomically corresponding to the striatum and cortex (center and right slices) and

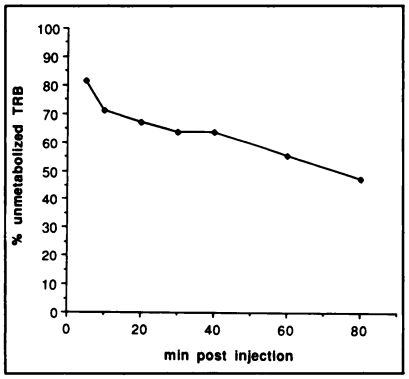

FIGURE 2. Fraction of monkey plasma total radioactivity which is unmetabolized [^{11}C]TRB at various time points following tracer injection. Results from one animal.

lowest in the cerebellum (lower portion of left slice). Scopolamine pretreatment resulted in a large reduction of [^{11}C]TRB uptake in cortex and striatum relative to that in the cerebellum. Representative time-activity curves of various brain regions of the pigtail monkey are shown in Figure 4. The ratio of left striatum (receptor-rich) to cerebellum (receptor-poor) tissue radioactivity measured from regions of interest was 3.5–4 at 50–80 min, and the left temporal cortex-to-cerebellum ratio over this time frame was approximately 3.

DISCUSSION

This study has examined the potential of [^{11}C]TRB as a PET receptor mapping agent using standard animal models. TRB was one of a series of compounds developed

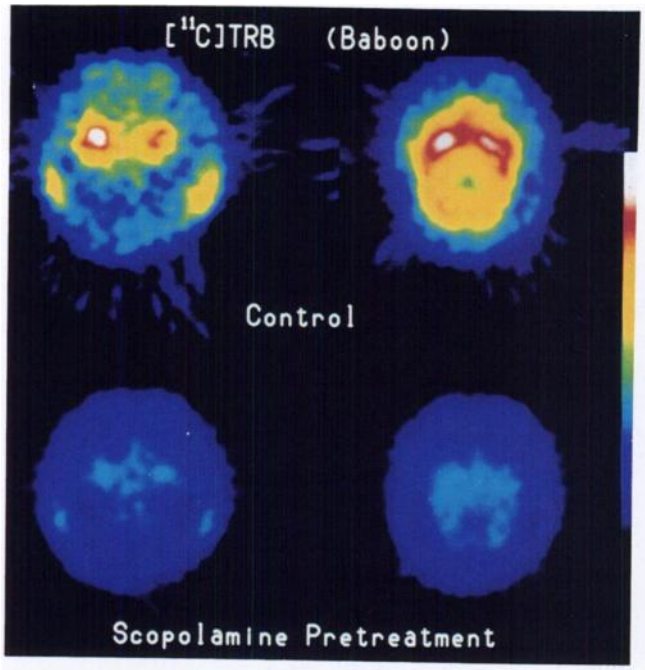

FIGURE 3. Eighty to 100-min transaxial PET images of [^{11}C] TRB radioactivity distribution in the same baboon brain before (top row) or following (bottom) scopolamine pretreatment. Brain levels are ascending from left to right. The slight asymmetry in cortical and subcortical areas is most likely an artifact caused by head movement or misalignment.

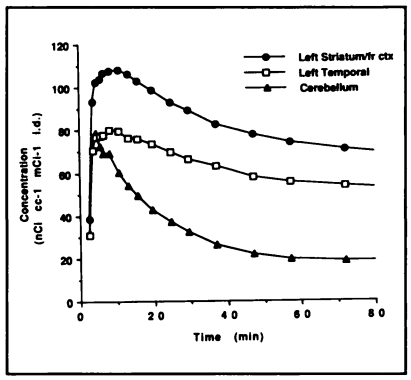

FIGURE 4. Representative time-tissue radioactivity curves for several brain regions measured by PET following intravenous injection of [^{11}C]TRB in a pigtail monkey.

originally as possible therapeutic agents for Parkinson's disease (*26*). It is a close chemical congener of QNB that penetrates the blood-brain barrier efficiently and possesses a high order of antimuscarinic potency (*26*) and receptor affinity. The IC_{50} value was 0.7 n*M* for (+)-TRB measured versus [^{3}H]QNB binding to mouse brain membrane preparations. This compares with IC_{50} values of 0.8 n*M* and 1.3 n*M* for (−)-QNB and scopolamine, respectively, under the same test conditions (*25*), and a reported IC_{50} for dexetimide of 3.3 n*M* (*13*). TRB appears to exhibit stereoselectivity in its actions since the (−) isomer of TRB has only about 10% of potency of the (+) isomer (*26*). The subtype specificity of TRB has not been studied, but it is likely to be similar to that of QNB and scopolamine, which both show high affinity for all mAChR subtypes. Unlike QNB, TRB possesses an N-methyl group that makes TRB fairly easy to label ^{11}C.

Tissue Biodistribution and Dosimetry

The high [^{11}C]TRB brain levels seen in rodents (3%–4% of the injected dose/brain at 30 min, Table 1) and primates (8%–12% peak amount, estimated from PET data) are noteworthy. In rats, [^{11}C]TRB radioactivity levels in the brain are 2–6 times greater than those of [^{11}C] scopolamine at similar times (Fig. 2) and about four-fold higher than the reported peak brain radioactive concentrations of [^{11}C]benztropine 30 min following injection into mice (*19*). Robust accumulation of tracer radioactivity in the imaging target area is an important characteristic in a PET agent because it maximizes the imaging signal for a given radiation dose. This is a particular concern with whole-body PET cameras which for geometry reasons are less sensitive than narrow diameter head-only units and therefore require more activity in the field of view. A corollary is that imaging agents with high tissue access can generally be administered in lower amounts with better dosimetry than agents with similar specificity but lower accessibility to the target tissue. The absorbed dose estimates for [^{11}C]TRB, based on its rat distribution, permit a cumulative adult human dose of 50 mCi of [^{11}C]TRB to be given. On the basis of studies presently underway in humans (*32*), it is estimated that this quantity is sufficient to permit three 16 mCi [^{11}C]TRB studies in the same individual using a Siemens-CTI 931 camera, with good count statistics at 60–90 min. Thus, sophisticated "test-retest" human studies are possible with [^{11}C]TRB.

Muscarinic Specificity

The demonstration of in vivo specificity and selectivity for binding sites is critically important in a potential receptor tracer. The regional brain and heart concentrations of [^{11}C]TRB at times beyond 30 min in rodents correlated well with known distributions of mAChR (*33, 34*). Highest localization occurred in the striatum and cortex and the striatum-to-cerebellum ratio increased in a nearly linear fashion over a 90-min period to values in the range of 10 for rat, to 13 (mouse, 60 min), with the increase being primarily due to clearance of tracer from cerebellum (Table 1). The prominent localization of [^{11}C]TRB in rodent brains at relatively short times is noteworthy in that it compares very favorably to, or exceeds that of several longer-lived isotope labeled ligands studied at substantially later time points, where the opportunity for clearance of nonspecific activity was greater. For instance, the rat caudate[striatum]/cerebellum ratios for [^{125}I]QNB and [^{3}H] QNB at 4 hr are 7 (*10*) and 8 (*35*), respectively; for [^{125}I] dexetimide the ratio in mice at 120 min is 10 (*13*), and the rodent ratios for [^{18}F]2- and 4-fluorodexetimides at 60 min have been variously reported as being between 6 and 25 (*15,16*).

PET measurements of brain regions in pigtail monkeys (n = 3) showed striatum (cortex)/cerebellum ratios of 3–4 from 50–80 min postinjection. This high degree of localization, measured externally at 13 mm resolution in a primate brain volume estimated to be less than 110 cm^3 (*36*), is an encouraging indicator for the use of [^{11}C]TRB in humans. It exceeds by approximately two-fold the baboon striatum-to-cerebellum ratio for [^{11}C]scopolamine under similar scan conditions (Frey et al., unpublished results), as well as that of [^{11}C]benztropine (1.5) measured at 6.0 mm resolution at 60 min (*19*).

Marked reductions of [^{11}C]TRB uptake in muscarinic tissues after pretreatment with pharmacological antagonists (Table 1, Figs. 1A and 3) is evidence for muscarinic specificity and saturability in the localization of this agent. The fact that the "receptor-poor" cerebellum also showed a 50% blockade (Table 1, Fig 1A) at first seems confusing, until it is remembered that nearly all regions of the brain contain some mAChR. Rat cerebellum contains about 8% of the concentration of mAChR found in the striatum (*34*). A quick inspection of the blocked and control 30-min rat [^{11}C]TRB data in Table 1 shows that the reduction in rat cerebellar [^{11}C]TRB concentration after blockade amounted to about 11% of the reduction in striatal [^{11}C] TRB concentration. The coincidence of these two measurements is intriguing and seems to further suggest high in vivo specificity for [^{11}C]TRB.

An alternate explanation for reduced tissue uptake following pretreatment is that poorly understood actions of the blocking drug unrelated to receptor occupation, such

as hemodynamic changes or stimulation of tracer disposition, might reduce tracer delivery to tissue. This possibility can be eliminated only after correcting the qualitative data of these studies by the true arterial input function. This was not done in the present work. However, the timing of pretreatments 30–90 min before tracer administration lessened the possibility that blood flow alterations or other acute effects of the blocking drug contributed in a major way to the observed dramatic changes in tracer uptake between control and pretreatment studies.

Metabolism

Labeled metabolites of a PET radiotracer must be absent from the target tissue in order to accurately quantify its tissue distribution following intravenous injection. Additionally, tracer metabolites in blood should be minimal, or well characterized through rapid analytical methods so that corrections can be made for radiolabeled metabolites in arterial blood. This study has found that [^{11}C]TRB is metabolized at a steady rate in rat and monkey, but no labeled metabolites are present in brain tissue. Furthermore, the large polarity difference between TRB and its labeled metabolites permits rapid and accurate analysis of unmetabolized [^{11}C]TRB in blood by simple solid-phase extraction, and a straighforward way of determining the true [^{11}C]TRB input function in human studies is thus available.

The liver, lung and kidney appear to be organs for metabolism and excretion of [^{11}C]TRB in rats, based upon these organs' significant radioactivity uptake and lack of uptake blockade by muscarinic antagonists. In fact, radioactivity levels in liver rose significantly after QNB (Fig. 1A), possibly because of increased circulating [^{11}C]TRB away from blocked tissues which normally would have served as sinks for muscarinic tracer. The fact that nearly 80% of the dose was still present in the rat body at 90 min (Table 2) suggests that, in this species at least, expiration of the label as metabolic $^{11}CO_2$ is a minor path. The wall of the small intestine retained significant concentrations of radioactivity (data not shown) that were not blockable with QNB. Although this organ is known to contain mAChR, analysis of intestinal tissue homogenates showed most of the radioactivity present here was not [^{11}C]TRB but instead polar or nonextractible metabolites.

The identities of the polar metabolites of [^{11}C]TRB in small intestine and blood are uncertain at this time. Their fairly rapid appearance and hydrophilic character suggest sulfate or glucuronide conjugate formation. A similar transformation is prominent in the metabolism of scopolamine in several mammal species (*37*). A speculation for the nonextractible intestinal ^{11}C-metabolite is [^{11}C]formaldehyde, produced in the liver by oxidative N-demethylation, then secreted through the bile duct to finally react covalently with proteins in the intestinal mucosa. The methyl group in [N-^{13}C-methyl]antipyrine shares a similar fate in the rat (*38*), and this route may be a common one for other ^{11}C-labeled N-methyl agents. Along these lines, moderate levels of nonextractible intestinal radioactivity have been observed following rat administration of several unrelated N-[^{11}C]methyl compounds (Mulholland, unreported results).

Synthesis

Although the fact is seldom stated, a potential PET tracer can have the opportunity for widespread use only if practical and reliable methods for its preparation are available. [^{11}C]TRB is a simple, stable molecule that can be produced routinely by standard [^{11}C]methyl iodide methylation in amounts greater than 250 mCi. In this respect, [^{11}C]TRB holds a clear advantage over [^{11}C]scopolamine and, with the possible exception of [^{11}C]benztropine (*19–21*), it also appears simpler to prepare than several other reported positron labeled central muscarinic tracers (*14–16*).

CONCLUSIONS

This study has found that [^{11}C]TRB has favorable uptake, dosimetry, muscarinic specificity and metabolism characteristics in animals, suggesting a promising mAChR mapping agent in humans. A final consideration, important to the eventual goal of single scan in vivo mAChR quantification, but beyond the scope of this report, is whether [^{11}C]TRB-tissue pharmacokinetics are "well-behaved" to the extent they can adequately be described by kinetic models used in PET for binding sites estimation under nonequilibrium study conditions (*10,22,23*).

Overall pharmacokinetics is a function of both the drug's properties and the characteristics of the particular tissue/receptor system, and to a significant degree is species-variable. The detailed distribution and kinetic behavior of [^{11}C]TRB in man constitute the final steps in validation of this agent as a radiopharmaceutical for muscarinic receptors. These investigations are underway and will be subjects of future reports.

ACKNOWLEDGMENTS

The authors are grateful to Teresa Pisani and Dr. Steven Papadopoulis for assistance in animal experiments, and to James Moskwa, Roger Lininger and John Caraher for operation of the cyclotron. Thanks are also due to Linder Markham for her help in preparing this manuscript. This work was supported by National Institutes of Health grants NS15655 and NS24896-04, and Department of Energy grant DE-FG02-87ER60528.

REFERENCES

1. Reinikainen KJ, Riekkinen PJ, Halonen T, Laakso M. Decreased muscarinic receptor binding in cerebral cortex and hippocampus in Alzheimer's disease. *Life Sci* 1987;41:453–461.
2. Bowen DM, Allen SJ, Benton JS, et al. Biochemical assessment of serotinergic and cholinergic dysfunction and cerebral atrophy in Alzheimer's disease. *J Neurochem* 1983;41:266–272.
3. Danielsson E, Eckernas S-A, Westlind-Danielsson A, et al. VIP-sensitive adenylate cyclase, guanylate cyclase, muscarinic receptors, choline acetyltransferase and acetylcholinesterase in brain tissue afflicated by Alzheimer's disease/senile dementia of the Alzheimer type. *Neurobiology of Aging*

1988;9:153–162.
4. Lange KW, Wells FR, Rossor MN, Jenner P, Marsden CD. Brain muscarinic receptors in Alzheimer's and Parkinson's disease. *Lancet* 1989;2:1279.
5. Whitehouse PJ, Trifiletti RR, Jones BE, et al. Neurotransmitter receptor alterations in Huntington's disease: autoradiographic and homogenate studies with special reference to benzodiazepine receptor complexes. *Ann Neurol* 1985;18:202–210.
6. Mizukawa K, Ogawa N, Sora YH, Sora I. Alterations of the muscarinic cholinergic (mACh) receptors in the striatum of the MPTP-induced parkinsonian model in mice: in vitro quantitative autoradiographical analysis. *Neurosci Lett* 1987;81:105–110.
7. Drayer B, Jaszczak R, Coleman E, et al. Muscarinic cholinergic receptor binding: in vivo depiction using single photon emission computed tomography and radioiodinated quinuclidinyl benzilate. *J Comput Assist Tomogr* 1982;6:536–543.
8. Eckelman WC, Reba RC, Rzeszotarski WJ, Gibson RE. External imaging of cerebral muscarinic acetylcholine receptors. *Science* 1984;223:291–293.
9. Eckelman WC, Eng R, Rzeszotarski WJ, Gibson RE, Francis B, Reba RC. Use of 3-quinuclidinyl 4-iodobenzilate as a receptor binding radiotracer. *J Nucl Med* 1985;26:637–642.
10. Gibson RE, Weckstein DJ, Jagoda EM, Rzeszotarski WJ, Reba RC, Eckelman WC. The characteristics of I-125 4-IQNB and H-3 QNB in vivo and in vitro. *J Nucl Med* 1984;25:214–222.
11. Holman BL, Gibson RE, Hill TC, Eckelman WC, Albert M, Reba RC. Muscarinic acetylcholine receptors in alzheimer's disease. In vivo imaging with iodine-123-labeled 3-quinuclidinyl-4-iodobenzilate and emission tomography. *JAMA* 1985;254:3063–3066.
12. Prenant C, Barre L, Crouzel C. Synthesis of [^{11}C]-3-quinuclidinylbenzilate (QNB). *J Labelled Cmpd Radiopharm* 1989;27:1257–1265.
13. Wilson AA, Dannals RF, Ravert HT, Frost JJ, Wagner Jr HN. Synthesis and biological evaluation of [^{125}I]- and [^{123}I]-4-iododexetimide, a potent muscarinic cholinergic receptor antagonist. *J Med Chem* 1989;32:1057–1062.
14. Dannals RF, Langstrom B, Ravert HT, Wilson AA, Wagner Jr HN. Synthesis of radiotracers for studying muscarinic cholinergic receptors in the living human brain using positron emission tomography: [^{11}C]dexetimide and [^{11}C]levetimide. *Appl Radiat Isot* 1988;39:291–295.
15. Wilson AA, Scheffel UA, Dannals RF, Stathis M, Ravert HT, Wagner Jr HN. In vivo biodistribution of two [18F]-labelled muscarinic cholinergic receptor ligands: 2-[18F]- and 4-[18F]-fluorodexetimide. *Life Sci* 1991;48:1385–1394.
16. Hwang D-R, Dence CS, McKinnon ZA, Mathias CJ, Welch MJ. Positron labeled muscarinic acetylcholine receptor antagonist 2- and 4-[^{18}F]fluorodexetimide: syntheses and biodistribution. *Nucl Med Biol* 1991;18:247–252.
17. Vora MM, Finn RD, Booth TE. [N-methyl-^{11}C]Scopolamine: synthesis and distribution in the rat brain. *J Labelled Compd Radiopharm* 1983;20:1229–1234.
18. Mulholland GK, Jewett DM, Toorongian SA. Routine synthesis of N-[^{11}C-methyl]scopolamine by phosphite mediated reductive methylation with [^{11}C]formaldehyde. *Appl Radiat Isot* 1988;39:373–379.
19. Dewey SL, MacGregor R, Brodie JD, et al. Mapping muscarinic receptors in human and baboon brain using [N-^{11}C-methyl]-benztropine. *Synapse* 1990;5:213–223.
20. Dewey SL, Brodie JD, Fowler JS, et al. Positron emission tomography (PET) studies of dopaminergic/cholinergic interactions in the baboon brain. *Synapse* 1990;6:321–327.
21. Dewey SL, Volkow ND, Logan J, et al. Age-related decreases in muscarinic cholinergic receptor binding in the human brain measured with positron emission tomography (PET). *J Neurosci Res* 1990;27:569–575.
22. Frey KA, Hichwa RD, Ehrenkaufer RLE, Agranoff BW. Quantitative in vivo receptor binding III: tracer kinetic modeling of muscarinic receptor binding. *Proc Natl Acad Sci USA* 1985;82:6711–6715.
23. Frey KA, Koeppe RA, Mulholland GK, et al. In vivo muscarinic cholinergic receptor imaging in human brain with [^{11}C]scopolamine and positron emission tomography. *Cereb Blood Flow Metab* 1991;12:147–154.
24. Mulholland GK, Otto CA, Jewett DM, et al. Radiosynthesis and comparisons in the biodistribution of carbon-11 muscarinic antagonists: (+)2a-tropanyl benzilate and N-methyl-4-piperidyl benzilate [Abstract]. *J Labelled Cmpd Radiopharm* 1989;27:202–203.
25. Otto CA, Mulholland GK, Perry SE, Combs R, Sherman PS, Fisher SJ. In vitro and ex vivo evaluation of cyclic aminoalkyl benzilates as potential emission tomography ligands for the muscarinic receptor. *Nucl Med Biol* 1989;16:51–55.
26. Atkinson ER, McRitchie DD, Shoer LF, et al. Parasympatholytic (anticholinergic) esters of the isomeric 2-tropanols. 1. Glycolates. *J Med Chem* 1977;20:1612–1617.
27. Archer S, Bell MR. U.S. Patent 3,145,210, 1964.
28. Crouzel C, Langstrom B. Pike VW, Coenen HH. Recommendations for a practical production of [^{11}C]methyl iodide. *Appl Radiat Isot* 1987;38:601–3.
29. Loevinger R, Berman M. A revised scheme for calculating absorbed dose from biologically distributed radionuclides. *MIRD Pamphlet No. 1, revised.* New York: Society of Nuclear Medicine; 1976.
30. Roedler H. Accuracy of internal dose calculations with special consideration of radiopharmaceuticals biokinetics. Radiopharmaceutical Dosimetry Symposium, Oak Ridge National Laboratory, HHS-Publ (FDA) 81-8166; 1980:1–20.
31. Watson E, Stabin M, Bolch W. *MIRDOSE2.* Oak Ridge Associated Universities, Oak Ridge, TN; 1988.
32. Frey KA, Koeppe RA, Mulholland GK, Kuhl DE. Quantification of regional cerebral muscarinic receptors in human brain with the use of [C-11]tropanyl benzilate and positron emission tomography [Abstract]. *J Nucl Med* 1990;31:885.
33. Yamamura HI, Snyder SJ. Muscarinic cholinergic binding in rat brain. *Proc Nat Acad Sci USA* 1974;71:1725–1729.
34. Birdsall NJM, Hulme EC, Burgen A. The character of the muscarinic receptors in different regions of the rat brain. *Proc R Soc Lond* 1980;B207:1–12.
35. Yamamura HI, Kuhar MJ, Snyder SJ. In vivo identification of muscarinic cholinergic receptor binding in rat brain. *Brain Res* 1974;80:170–176.
36. Parker ST. "Why big brains are so rare." In: Parker ST, Gibson KR, eds. *Language and intelligence in monkeys and apes.* Cambridge: University Press; 1990;129–154.
37. Werner VG, Schmidt K-H. Chemische Analyse des Stoffwechels von (−)-Scopolamin bei einigen Saugetieren. *Hoppe-Seyler's Z Physiol Chem* 1968;349:741–752.
38. Huetter P, Albert K, Bayer E, Zeller KP, Hartmann F. Generation of formaldehyde by N-demethylation of antipyrine. *Biochem Pharmacol* 1987;36:2729–2733.